Eur. Phys. J. C 53, 205–213 (2008)
DOI 10.1140/epjc/s10052-007-0479-0

THE EUROPEAN PHYSICAL JOURNAL C

Regular Article – Experimental Physics

Possible implications of the channeling effect in NaI(Tl) crystals

R. Bernabei[1,a], P. Belli[1], F. Montecchia[1], F. Nozzoli[1], F. Cappella[2], A. Incicchitti[2], D. Prosperi[2], R. Cerulli[3], C.J. Dai[4], H.L. He[4], H.H. Kuang[4], J.M. Ma[4], X.H. Ma[4], X.D. Sheng[4], Z.P. Ye[4,5], R.G. Wang[4], Y.J. Zhang[4]

[1] Dip. di Fisica, Università di Roma Tor Vergata and INFN, sez. Roma Tor Vergata, 00133 Rome, Italy
[2] Dip. di Fisica, Università di Roma La Sapienza and INFN, sez. Roma, 00185 Rome, Italy
[3] Laboratori Nazionali del Gran Sasso, INFN, Assergi, Italy
[4] IHEP, Chinese Academy, P.O. Box 918/3, Beijing 100039, P.R. China
[5] University of Jing Gangshan, Jiangxi, P.R. China

Received: 1 October 2007 /
Published online: 28 November 2007 –

Abstract. The channeling effect of low energy ions along the crystallographic axes and planes of NaI(Tl) crystals is discussed in the framework of corollary investigations on WIMP dark matter candidates. In fact, the modeling of this existing effect implies a more complex evaluation of the luminosity yield for low energy recoiling Na and I ions. In the present paper related phenomenological arguments are developed and possible implications are discussed at some extent.

PACS. 95.35.+d

1 Introduction

It is known that ions (and, thus, also recoiling nuclei) move in a crystal in a different way than in amorphous materials. In particular, ions moving (quasi-) parallel to crystallographic axes or planes feel the so-called "channeling effect" and show an anomalous deep penetration into the lattice of the crystal [1–4]; see Fig. 1.

For example, already on 1957, a penetration of $^{134}Cs^{+}$ ions into a Ge crystal was observed to a depth of about 1000 Å [5], larger than that expected in the case the ions would cross amorphous Ge ($\simeq 50$ Å). Afterwards, high intensities of H^{+} ions at 75 keV transmitted through thick (3000–4000 Å) single-crystal gold films in the $\langle 110 \rangle$ directions were detected [2]. Other examples for keV range ions have been shown in [6] where 3 keV P^{+} ions moving into layers of 500 Å of various crystals were studied.

The channeling effect is also exploited in high energy physics e.g. to extract high energy ions from a beam by means of bent crystals or to study diffractive physics by analysing scattered ions along the beam direction (see e.g. [7]).

Recently [8] it has been pointed out the possible role which this effect can play in the evaluation of the detected energy of recoiling nuclei in crystals, such as the NaI(Tl).[1]

In fact, the channeling effect can occur in crystalline materials due to correlated collisions of ions with target atoms. In particular, the ions through the open channels have ranges much larger than the maximum range they would have if their motion would be either in other directions or in amorphous materials. Moreover, when a low-energy ion goes into a channel, its energy losses are mainly due to the electronic contributions. This implies that a channeled ion transfers its energy mainly to electrons rather than to the nuclei in the lattice and, thus, its quenching factor (namely the ratio between the detected energy in keV electron equivalent [keVee] and the kinetic energy of the recoiling nucleus in keV) approaches the unity.

It is worth to note that this fact can have a role in corollary analyses in the dark matter particle direct detection experiments, when WIMP (or WIMP-like) candidates are considered. In fact, since the routine calibrations of the detectors are usually performed by using γ sources (in order to avoid induced radioactivity in the materials), the quenching factor is a key quantity to derive the energy of the recoiling nucleus after an elastic scattering. Generally, for scintillation and ionization detectors this factor has been inferred so far by inducing tagged recoil nuclei through neutron elastic scatterings[2]; however, as it will be discussed in Sect. 3, the usual analysis carried out on similar measurements does not allow to account for the channeled events. A list of similar values for various nuclei in different detectors can be found e.g. in [10]. In particular,

[a] e-mail: rita.bernabei@roma2.infn.it

[1] For completeness, it is worth to note that luminescent response for channeling in NaI(Tl) was already studied in [9] for MeV-range ions.

[2] for a review see Table X of [10]

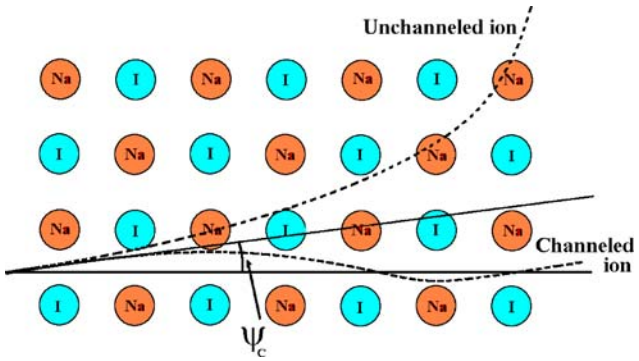

Fig. 1. Simplified schema of the channeling effect in the NaI(Tl) lattice. The axial channeling occurs when the angle of the motion direction of an ion with the respect to the crystallographic axis is less than a characteristic angle, Ψ_c, depicted there (see for details Sect. 2). Two examples for channeled and unchanneled ions are also shown (*dashed lines*)

commonly in the interpretation of the dark matter direct detection results in terms of WIMP (or WIMP-like) candidates the quenching factors are assumed to be constant values without considering e.g. their energy dependence, the properties of each specific used detector and the experimental uncertainties. An exception was in the DAMA/NaI corollary model dependent analyses for WIMP (or WIMP-like) candidates [10–13] where at least some of the existing uncertainties on the $q_{\rm Na}$ and $q_{\rm I}$ values, measured with neutrons, were included.

In this paper the possible impact of the channeling effect in NaI(Tl) crystals is discussed in a phenomenological framework and comparisons on some of the corollary analyses carried out in terms of WIMP (or WIMP-like) candidates [10–13], on the basis of the 6.3 σ C.L. DAMA/NaI model independent evidence for particle dark matter in the galactic halo[3], are given.

2 Luminosity, range and channeling in NaI(Tl) crystals

The stopping power of an ion inside an amorphous material is given by the sum of two effects: its interaction with the nuclei (n) of the material and its interaction with the binding electrons (e) [33].

If E is the energy of the ion at any point x along the path, its stopping power can be written as:

$$\frac{{\rm d}E_{\rm ion}}{{\rm d}x}(E) = \frac{{\rm d}E_{{\rm ion}-n}}{{\rm d}x}(E) + \frac{{\rm d}E_{{\rm ion}-e}}{{\rm d}x}(E)\,, \qquad (1)$$

where $\frac{{\rm d}E_{{\rm ion}-n}}{{\rm d}x}$ and $\frac{{\rm d}E_{{\rm ion}-e}}{{\rm d}x}(E)$ are the nuclear and the electronic stopping powers of the ion, respectively. They can be evaluated – following the theory firstly developed in [33] – by using some available packages, as the SRIM code [34].

We have to stress that the detectable light produced by a charged particle (either electron or ion) in scintillator detectors mostly arises from the energy loss in the electronic interactions. Thus, the differential luminosities in scintillators, $\frac{{\rm d}L_e}{{\rm d}x}$ and $\frac{{\rm d}L_{\rm ion}}{{\rm d}x}$ for electrons and ions, respectively, can be written as:

$$\begin{aligned}
\frac{{\rm d}L_e}{{\rm d}x} &= \alpha \frac{{\rm d}E_{e-e}}{{\rm d}x} && \text{for electrons} \\
\frac{{\rm d}L_{\rm ion}}{{\rm d}x} &= \alpha \frac{{\rm d}E_{{\rm ion}-e}}{{\rm d}x}(E) \\
&= \alpha \times \frac{{\rm d}E_{\rm ion}}{{\rm d}x} \times q'(E) && \text{for ions (recoils)}
\end{aligned} \qquad (2)$$

where α is a proportionality constant, $\frac{{\rm d}E_{e-e}}{{\rm d}x}$ is the stopping power of an electron in the material and

$$q'(E) = \left(\frac{{\rm d}E_{{\rm ion}-e}}{{\rm d}x}(E)\right) \Big/ \left(\frac{{\rm d}E_{{\rm ion}-n}}{{\rm d}x}(E) + \frac{{\rm d}E_{{\rm ion}-e}}{{\rm d}x}(E)\right)$$

is defined as "differential quenching factor".

The total detected luminosities, $L = \int_{\rm path} \frac{{\rm d}L}{{\rm d}x}\,{\rm d}x$, for electrons and ions can be written in the form:

$$\begin{aligned}
L_e &= \alpha \int_{\rm path} \frac{{\rm d}E_{e-e}}{{\rm d}x}\,{\rm d}x = \alpha E_e && \text{for electrons} \\
L_{\rm ion} &= \alpha \int_{\rm path} q'(E) \times \frac{{\rm d}E_{\rm ion}}{{\rm d}x}\,{\rm d}x \\
&\equiv \alpha \times q_1(E_{\rm ion}) \times E_{\rm ion} && \text{for ions (recoils)}\,,
\end{aligned} \qquad (3)$$

in addition, the range of an ion is:

$$\begin{aligned}
{\rm R}_{\rm ion}(E) &= \int_0^E \frac{{\rm d}E'}{{\rm d}E_{\rm ion}/{\rm d}x} \equiv q_2(E) \times \int_0^E \frac{{\rm d}E'}{{\rm d}E_{{\rm ion}-e}/{\rm d}x} \\
&= q_2(E) \times \mathbf{R}_e(E)\,.
\end{aligned} \qquad (4)$$

In (3) and (4) $q_1(E) = \frac{1}{E}\int_0^E q'(E')\,{\rm d}E'$ is the "light quenching factor" and $q_2(E) = \int_0^E \frac{{\rm d}E'}{{\rm d}E_{\rm ion}/{\rm d}x} / \int_0^E \frac{{\rm d}E'}{{\rm d}E_{{\rm ion}-e}/{\rm d}x}$ is the "range quenching factor". In the energy region of interest for the dark matter detection $q_1(E) \simeq q_2(E)$ within 10%–20%. In particular, the values of the quenching factors for recoiling nuclei in detectors made of amorphous materials are well below the unity in the keV energy region.

The situation changes when the detector is either a crystal or a multi-crystalline material (the size of a single crystal has to be larger than few thousands of Å). In this case the luminosity depends on whether the recoiling nucleus is (quasi-) parallel to the crystallographic axes or planes or not. In the first case, since the energy losses of the ion are mainly due to the electronic contributions, the penetration (and the range) of the ion becomes much larger, of the order of $\mathbf{R}_e$, and the quenching factor approaches the unity.

[3] We remind that various possibilities for some of the many possible astrophysical, nuclear and particle physics scenarios have have been analysed by DAMA itself both for some WIMP/WIMP-like candidates and for light bosons [10–14], while other corollary analyses are also available in literature, such as e.g. [8, 15–32]. Many other scenarios can be considered as well.

The theory of ion channeling in crystals has been developed e.g. in [3, 4, 35]. In particular, this theory deals with channeling of low energy, high mass ions as a separate case from high energy, low mass ions. Here, we only remind that the condition for a low energy ion and a recoiling nucleus to be axially channeled along a certain string of atoms in the lattice is linked to a critical angle, $\Psi_{\rm c}$ (see Fig. 1); for details refer to [3, 4, 35]. When the ion (recoiling nucleus) has a moving direction with an angle Ψ with respect to this string lower than $\Psi_{\rm c}$, it is axially channeled.

The critical angles for axial channeling is given by [3, 4, 35]:

$$\Psi_{\rm c} = \sqrt{\frac{C a_{\rm TF}}{d\sqrt{2}}\Psi_1}\,, \tag{5}$$

where $C^2 \simeq 3$ is the Lindhard's constant and d is the inter-atomic spacing in the crystal along the channeling direction. The Thomas–Fermi radius, $a_{\rm TF}$, can be written as [3, 4, 35]:

$$a_{\rm TF} = \frac{0.8853 a_0}{\left(\sqrt{Z_1}+\sqrt{Z_2}\right)^{2/3}}\,, \tag{6}$$

where Z_1 and Z_2 are the atomic numbers of the projectile (recoiling nucleus) and target atoms, respectively; $a_0 = 0.529$ Å is the Bohr radius.

The characteristic angle Ψ_1 is defined as a function of the ion (recoiling nucleus) energy, E, by:

$$\Psi_1 = \sqrt{\frac{2Z_1 Z_2 e^2}{Ed}}\,, \tag{7}$$

where e is the electron's charge. The condition $\Psi < \Psi_{\rm c}$ for axial channeling is valid for $\Psi_1 > \Psi_{1,\rm lim} = \frac{a_{\rm TF}}{d}$, that is for $E < E_{\rm lim} = \frac{2Z_1 Z_2 e^2 d}{a_{\rm TF}^2}$ [3, 4, 35]. Hence, typical values for NaI(Tl) crystal assure that for recoil's energies less than 170 keV the quoted formulas hold. For completeness, we just remind that it has also been suggested that the critical angles may slightly depend on the temperature [36]. Moreover, the critical angles at low energy have a weaker dependence on ion energy than those at higher energy. In fact, at higher energy, the critical angle is $\simeq C\Psi_1$ [3, 4, 35].

In the case of planar channeling for low energy ions the critical angle can be written as [37] (see also [35]):

$$\theta_{\rm pl} = a_{\rm TF}\sqrt{N d_{\rm p}}\left(\frac{Z_1 Z_2 e^2}{E a_{\rm TF}}\right)^{1/3}, \tag{8}$$

where N is the atomic number density and $d_{\rm p}$ is the interplane spacing. The dependence of $\theta_{\rm pl}$ on the energy is weaker than that at higher energy, where it can be written as [7, 38]:

$$\theta_{\rm pl} = a_{\rm TF}\sqrt{N d_{\rm p}}\left(\frac{2Z_1 Z_2 e^2 C}{E a_{\rm TF}}\right)^{1/2}. \tag{9}$$

Taking into account the critical angles for axial and planar channeling in NaI(Tl), we have calculated by Monte Carlo method the solid angle interested by both axial and planar channeling in NaI(Tl) crystals as a function of the energy of the recoiling nuclei, $E_{\rm R}$; see Fig. 2. Moreover, just the lower index crystallographic axes and planes have been considered, for the axial channeling: ⟨100⟩, ⟨110⟩, ⟨111⟩ and for the planar channeling: {100}, {110}, {111}.

In this way, the estimated light response of a NaI(Tl) crystal scintillator to sodium and iodine recoils at given energy has been studied taking into account the channeling effect in the considered modeling. For a given nucleus A with recoil energy $E_{\rm R}$ the response of a NaI(Tl) crystal scintillator can be written as $\frac{{\rm d}N_A}{{\rm d}E_{\rm det}}(E_{\rm det}|E_{\rm R})$, where $E_{\rm det}$ is the detected energy. By the definition: $\int_0^\infty \frac{{\rm d}N_A}{{\rm d}E_{\rm det}}(E_{\rm det}|E_{\rm R})\,{\rm d}E_{\rm det} = 1$. In most cases of the dark matter direct detection field – that is without including the channeling effect – the light response is assumed equal to a Dirac delta function:

$$\frac{{\rm d}N_A}{{\rm d}E_{\rm det}}(E_{\rm det}|E_{\rm R}) = \delta(E_{\rm det} - q_A E_{\rm R})\,,$$

where q_A is the value (assumed constant) of the quenching factor of the unchanneled A nucleus recoils.

The evaluation of $\frac{{\rm d}N_A}{{\rm d}E_{\rm det}}$, when accounting for channeling effect, has been realised by means of a Monte Carlo code; the path of a recoiling nucleus, at a given recoil energy $E_{\rm R}$, has been calculated under the following reasonable and cautious assumptions:

(i) isotropic distribution of the recoils;

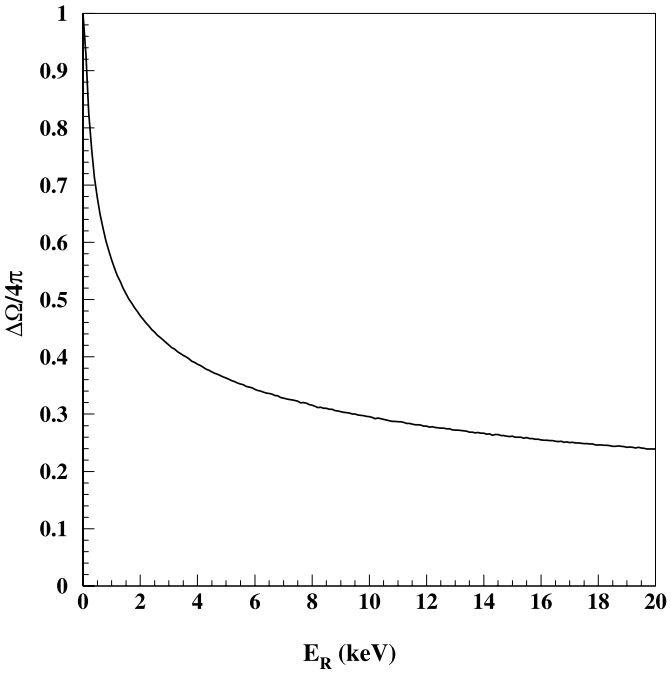

Fig. 2. Fraction of solid angle interested by both axial and planar channeling in NaI(Tl) crystals as a function of the energy of the recoiling nuclei, calculated according to the text. In these calculations just the lower index crystallographic axes and planes have been considered: for the axial channeling: ⟨100⟩, ⟨110⟩, ⟨111⟩ and for the planar channeling: {100}, {110}, {111}

(ii) in the case the recoil would enter in a channel, a de-channeling can occur due to some interactions with impurities in the lattice, as Tl luminescent dopant centers. The probability density of such a process is assumed to be: $p(x) = \frac{1}{\lambda} e^{-x/\lambda}$, with $\lambda = 1200$ Å, that is the average distance among the Tl centers;
(iii) the energy losses by the recoil nuclei in a channel just depend on the electronic stopping power (see (1));
(iv) the energy losses by the recoil nuclei in a channel are converted into scintillation light with a quenching factor ~ 1;
(v) if a recoil is de-channeled due to a nuclear interaction, it can either re-enter into another channel or not. The differential distribution of the nuclear interaction is assumed to be isotropic;
(vi) in case the recoil would not enter into a channel, it is cautiously assumed that it stops and its released energy is converted into scintillation light with the quenching factor of unchanneled events. In this case the straggling is considered as evaluated by the SRIM code [34].

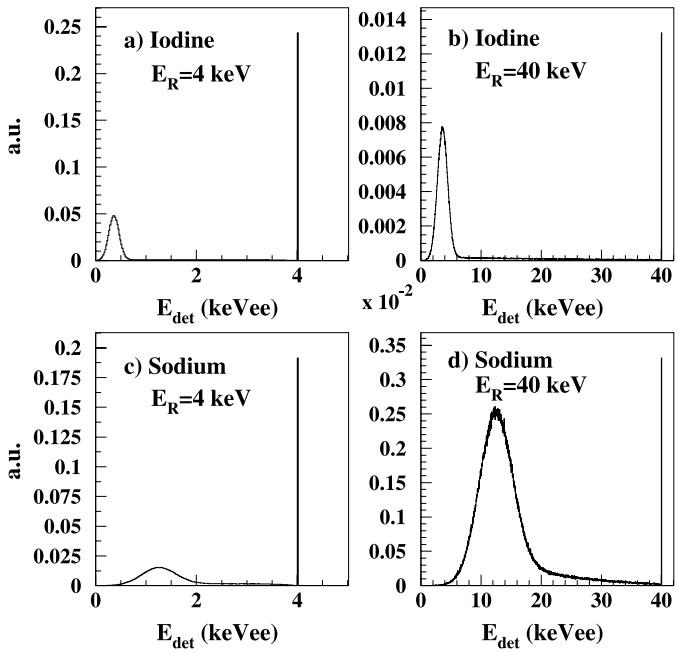

Fig. 3. Examples of light responses in terms of keVee, $\frac{dN_A}{dE_{det}}(E_{det}|E_R)$, for iodine recoils of 4 keV **a** and of 40 keV **b** and for sodium recoils of 4 keV **c** and of 40 keV **d** in the modeling given in the text. In this calculation the quenching factors for sodium and iodine recoils in amorphous or out of channel NaI(Tl) are assumed at the mean values given in [39]. Just to emphasize the effect of the channeling, the broadening due to the energy resolution of the detector has not been included here. The peaks corresponding to fully channeled events ($q \sim 1$) and to fully quenched events (broadened by the straggling) are well evident; in the middle events, which have been de-channeled at least once, are also visible. It is possible to note that e.g. in the case of iodine recoils the fully channeled events are about 25% at 4 keV; this percentage becomes smaller, about 1% at 40 keV

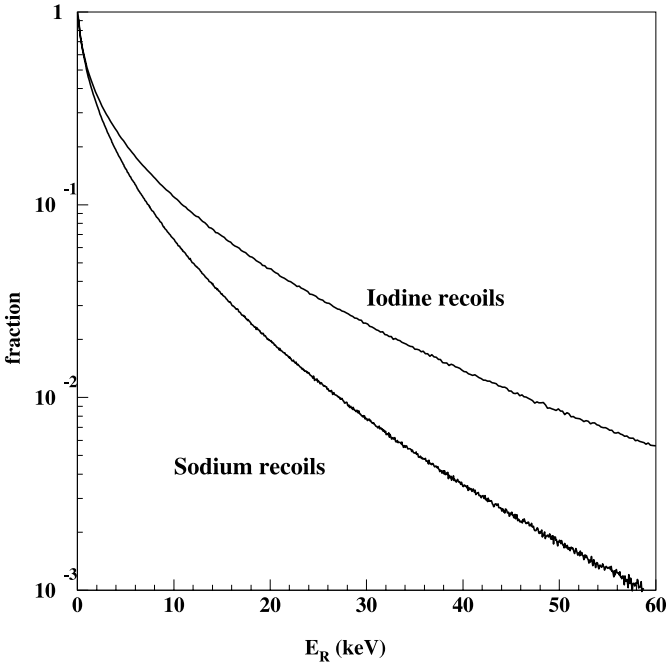

Fig. 4. Fraction of events with quenching factor $\simeq 1$, that is fully channeled events, as a function of the energy of the recoiling nuclei in NaI(Tl) crystals according to the modeling described in the text

In Fig. 3 few examples of light responses in terms of keVee for Iodine recoils of 4 keV (a) and of 40 keV (b) and for Sodium recoils of 4 keV (c) and of 40 keV (d) are given. In these calculations the quenching factors for sodium and iodine recoils in amorphous or out of channel NaI(Tl) are assumed at the mean values given in [39]. Just to emphasise the effect of the channeling, the broadening due to the energy resolution of the detector has not been included in this figure. The peaks corresponding to fully channeled events ($q \sim 1$) and to fully quenched events (broadened by the straggling) are well evident; in the middle events, which have been de-channeled at least once, are also visible.

Finally, in Fig. 3 it is possible to note that the number of fully channeled ($q \sim 1$) events strongly decreases when increasing the recoil energy: they are $\sim 25\%$ at 4 keV and $\sim 1\%$ at 40 keV for Iodine recoils and $\sim 18\%$ at 4 keV and $\sim 0.3\%$ at 40 keV for Sodium recoils. These behaviours are depicted in Fig. 4.

3 Some comments

Let us now analyse the phenomenologies connected both with the data on nuclear recoils induced by neutron scatterings and with the WIMP (or WIMP-like) direct detection in the light of the presence of the channeling effect.

In particular, Fig. 5 shows some examples of neutron calibrations of NaI(Tl) detectors at relatively low recoil energy. There the energy responses of the used

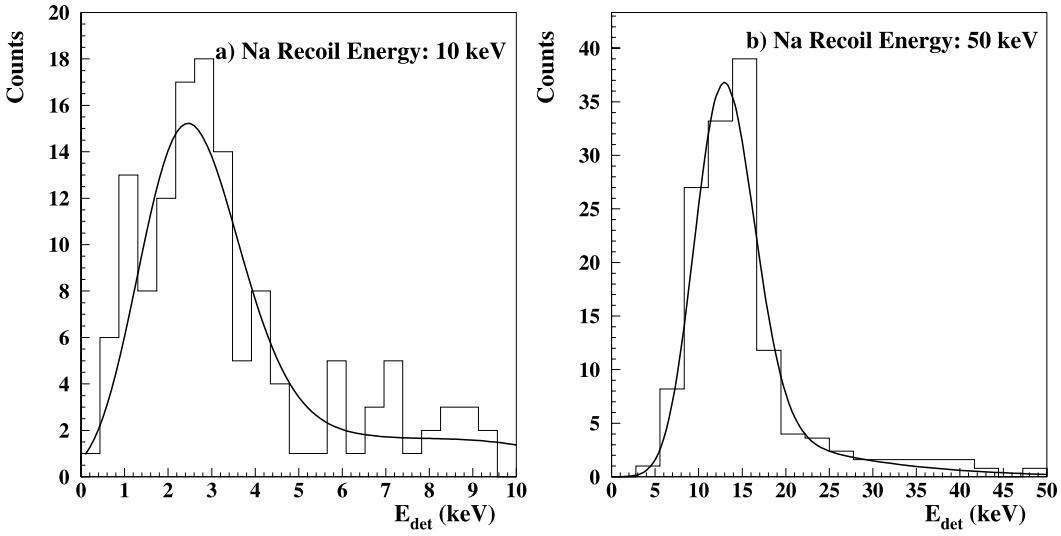

Fig. 5. Examples of neutron calibrations of NaI(Tl) detectors at low recoil energy. In particular, the energy responses of NaI(Tl) detectors to sodium recoils of 10 keV (*left panel*) [40] and of 50 keV (*right panel*) [41] are shown; the *peaks* corresponding to the quenched events are well clear. The superimposed continuous curves have been calculated as those of Fig. 3, obviously broadening them by the energy resolution of the corresponding detector. The fully channeled peaks ($q \sim 1$), which contain in these cases only the 6% and 0.15% of the events respectively, are smeared out by the energy resolution and can just contribute to the higher energy tails in the energy spectra

NaI(Tl) detectors to Sodium recoils of 10 keV [40] and of 50 keV [41] are reported as solid histograms; the peaks corresponding to the quenched events are well clear. The superimposed continuous curves have been calculated as those of Fig. 3, obviously broadening them by the energy resolution of the corresponding detector. The fully channeled peaks ($q \sim 1$), which in these cases can contain only the 6% and 0.15% of the events respectively (see Fig. 4), are smeared out by the energy resolution and only contribute to the higher energy tails in the energy spectra.

Thus, the simple analysis of Fig. 5 shows that the neutron data can contain channeled events, but – owing to the low-statistics of these measurements, to the small effect looked for and to the energy resolution – they cannot easily be identified. Moreover, as already shown, the channeling effect becomes less important at increasing energy and gives more suppressed contributions in the neutron scattering data. For Iodine recoils the situation is even worse. Therefore, there is no hope to single out the channeling effect in the already-collected neutron data.

On the other hand, the accounting of the channeling effect can give a significant impact in the sensitivities of the dark matter direct detection methods when WIMP (or WIMP-like) candidates are considered. In particular in Sects. 4 and 5 we will show that lower cross sections are explorable in given models for WIMP and WIMP-like candidates by crystal scintillators, such as NaI(Tl) (up to more than a factor 10 in some mass range). Moreover:

(i) similar situation holds for purely ionization detectors, as Ge (HD-Moscow – like experiments);
(ii) the loss of sensitivity occurs when pulse shape discrimination is used in crystal scintillators (KIMS); in fact, the channeled events ($q \simeq 1$) are probably lost;
(iiii) no enhancement can be present in liquid noble gas experiments (DAMA/LXe, WARP, XENON, ...);
(iv) no enhancement is possible for bolometer experiments; on the contrary some loss of sensitivity is expected since events (those with $q_{\rm ion} \simeq 1$) are lost by applying some discrimination procedures, based on $q_{\rm ion} \ll 1$.

4 Application to the WIMP-nucleus elastic scattering

Let us now consider the case of WIMP (or WIMP-like) elastic scattering on target nuclei. In particular, the expected differential counting rate of recoils induced by WIMP-nucleus elastic scatterings has to be evaluated in given astrophysical, nuclear and particle physics scenarios, also requiring assumptions on all the parameters involved in the calculations and the proper consideration of the related uncertainties (for some discussions see e.g. [10–14]). Hence, the proper accounting for the channeling effects must be considered as an additional uncertainties in the evaluation of the expected differential counting rate. The usual hypothesis that just one component of the dark halo can produce elastic scatterings on nuclei will be assumed here. In addition, the presence of the existing Migdal effect and the possible SagDEG contribution – we discussed in [13] and [12] respectively – will be not included here for simplicity. Thus, for every target specie A, the

expected distribution of the detected energy can be written as a convolution between the light response function, $\frac{\mathrm{d}N_A}{\mathrm{d}E_{\rm det}}$, defined in the previous section, and the differential distribution produced in the WIMP-nucleus elastic scattering:

$$\frac{\mathrm{d}R_A^{(\rm ch)}}{\mathrm{d}E_{\rm det}}(E_{\rm det}) = \int \frac{\mathrm{d}N_A}{\mathrm{d}E_{\rm det}}(E_{\rm det}|E_{\rm R})\frac{\mathrm{d}R_A}{\mathrm{d}E_{\rm R}}(E_{\rm R})\,\mathrm{d}E_{\rm R}\,. \tag{10}$$

The differential energy distribution of recoils, as function of the recoil energy $E_{\rm R}$, is:

$$\frac{\mathrm{d}R_A}{\mathrm{d}E_{\rm R}}(E_{\rm R}) = N_{\rm T}\frac{\rho_{\rm W}}{m_{\rm W}}\int_{v_{\rm min}(E_{\rm R})}^{v_{\rm max}} \frac{\mathrm{d}\sigma}{\mathrm{d}E_{\rm R}}(v, E_{\rm R})vf(v)\,\mathrm{d}v\,. \tag{11}$$

In this formula:

(i) $N_{\rm T}$ is the number of target nuclei of A specie;
(ii) $\rho_{\rm W} = \xi\rho_0$, where ρ_0 is the local halo density and $\xi \leq 1$ is the fractional amount of local WIMP density;
(iii) $m_{\rm W}$ is the WIMP mass;
(iv) $f(v)$ is the WIMP velocity (v) distribution in the Earth frame;
(v) $v_{\rm min} = \sqrt{\frac{m_A \cdot E_{\rm R}}{2m_{WA}^2}}$ (m_A and m_{WA} are the nucleus mass and the reduced mass of the WIMP-nucleus system, respectively);
(vi) $v_{\rm max}$ is the maximal WIMP velocity in the halo evaluated in the Earth frame;
(vii) $\frac{\mathrm{d}\sigma}{\mathrm{d}E_{\rm R}}(v, E_{\rm R}) = \left(\frac{\mathrm{d}\sigma}{\mathrm{d}E_{\rm R}}\right)_{\rm SI} + \left(\frac{\mathrm{d}\sigma}{\mathrm{d}E_{\rm R}}\right)_{\rm SD}$, with $\left(\frac{\mathrm{d}\sigma}{\mathrm{d}E_{\rm R}}\right)_{\rm SI}$ spin independent (SI) contribution and $\left(\frac{\mathrm{d}\sigma}{\mathrm{d}E_{\rm R}}\right)_{\rm SD}$ spin dependent (SD) contribution.

Finally, the expected differential counting rate as a function of the detected energy, $E_{\rm det}$, for a real multiple-nuclei detector (as e.g. the NaI(Tl)) when taking into account the channeling effect can easily be derived by summing the (10) over the nuclei species and accounting for the detector energy resolution:

$$\frac{\mathrm{d}R_{\rm NaI}^{(\rm ch)}}{\mathrm{d}E_{\rm det}}(E_{\rm det}) = \int G(E_{\rm det}, E') \sum_{A={\rm Na,I}} \frac{\mathrm{d}R_A^{(\rm ch)}}{\mathrm{d}E'}(E')\,\mathrm{d}E'\,. \tag{12}$$

The $G(E_{\rm det}, E')$ kernel generally has a Gaussian behaviour.

Few examples of shapes of expected energy distributions with and without accounting for the channeling effect, calculated in the modeling given above, are shown in Fig. 6. For this template purpose – accounting also for the experimental features of the detectors [10, 11, 42, 43] – we have just adopted the following additional assumptions (among all the many possibilities):

(i) mass of $m_{\rm W} = 20$ GeV;
(ii WIMP with dominant spin independent coupling and with nuclear cross sections $\propto A^2$;
(iii) point-like SI cross section $\sigma_{\rm SI} = 10^{-6}$ pb;
(iv) an halo model NFW (identifier A5 in [44], local velocity $v_0 = 220$ km/s and halo density at the maximum value 0.74 GeVcm^{-3} [44];
(v) form factors and quenching factors of ^{23}Na and ^{127}I as in case A of [10].

These pictures point out the enhancement of the sensitivity due to the channeling effect according to the given modeling.

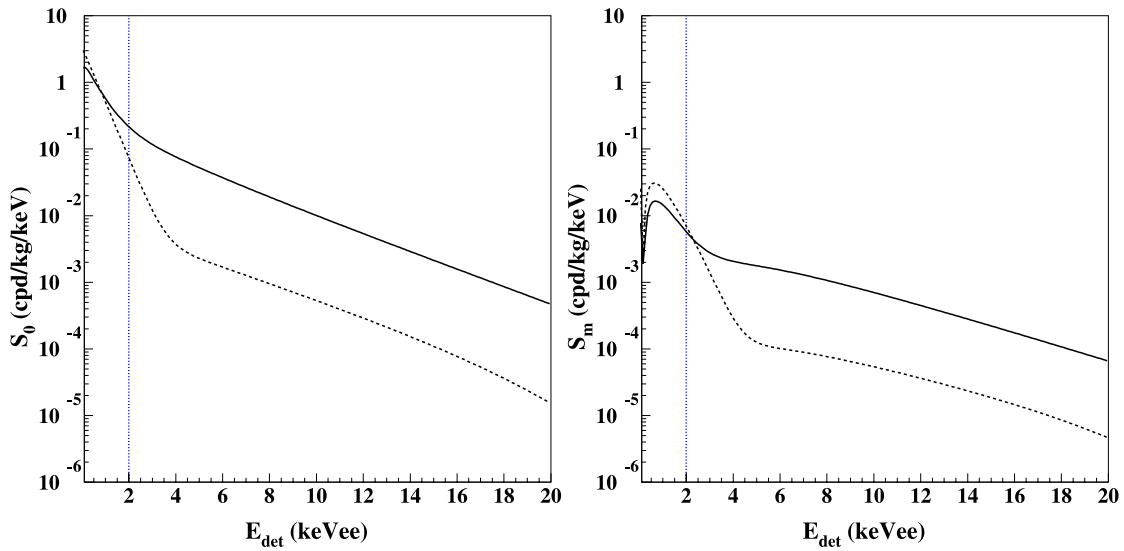

Fig. 6. An example of the shapes of the expected energy distributions in NaI(Tl) from sodium and iodine recoils induced by WIMP interactions with (*continuos line*) and without (*dashed line*) including the channeling effect in the crystal for the scenario given in the text. *Left panel*: behaviour of the unmodulated part of the expected signal, S_0. *Right panel*: behaviour of the modulated part of the expected signal, $S_{\rm m}$. The *vertical lines* indicate the energy threshold of the DAMA/NaI experiment

5 Examples of the possible impact on some corollary quests from the DAMA/NaI data

The accounting of the channeling effect in corollary quests for WIMPs as dark matter candidate particles can be investigated by exploiting the expected energy distribution, derived above, to some of the previous analyses on the DAMA/NaI annual modulation data in terms of WIMP-nucleus elastic scattering. For this purpose, the same scaling laws and astrophysical, nuclear and particles physics frameworks of [10, 11] are adopted. In addition, as already mentioned, for simplicity just to point out the impact of the channeling effect, the possible SagDEG contribution to the galactic halo and the presence of the existing Migdal effect – whose effects we discussed in [12] and [13], respectively – will not be included here.

The results for each kind of interaction are presented in terms of allowed volumes/regions, obtained as superposition of the configurations corresponding to likelihood function values *distant* more than 4σ from the null hypothesis (absence of modulation) in each one of the several (but still a very limited number) of the considered model frameworks. This allows us to account – at some extent – for at least some of the existing theoretical and experimental uncertainties (see e.g. in [10–14] and in the related astrophysics, nuclear and particle physics literature). Here only the low mass volumes/regions, where the channeling effect is dominant, are depicted.

Since the ^{23}Na and ^{127}I are fully sensitive both to SI and to SD interactions, the most general case is defined in a four-dimensional space $(m_{\rm W}, \xi\sigma_{\rm SI}, \xi\sigma_{\rm SD}, \theta)$, where: i) $\sigma_{\rm SI}$ is the point-like SI WIMP-nucleon cross section and $\sigma_{\rm SD}$ is the point-like SD WIMP-nucleon cross section, according to the definitions and scaling laws considered in [10]; ii) $tg\theta$ is the ratio between the effective coupling strengths to neutron and proton for the SD couplings (θ can vary between 0 and π) [10].

Preliminarily, here to offer an example of the impact of accounting for the channeling effect as given in the text, Fig. 7 shows a comparison for allowed slices corresponding to purely SI coupled WIMPs in some particular given scenario. This example has been evaluated for an halo model Evans' logarithmic with $R_{\rm c} = 5$ kpc (identifier A1 in [44]) for a v_0 value of 170 km/s and halo density at

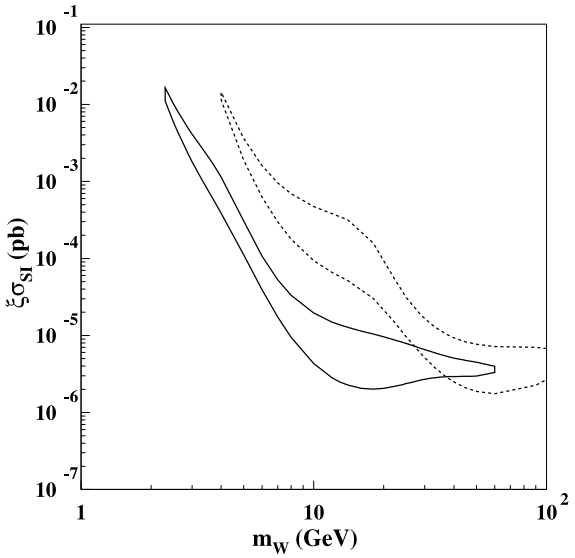

Fig. 7. An example of the effect of the channeling, modelled as in the text, on a DAMA/NaI allowed region for purely SI coupling WIMPs in the given scenario (see text). The region encloses configurations corresponding to likelihood function values *distant* more than 4σ from the null hypothesis (absence of modulation). This example has been evaluated according to the assumptions given in the text. In particular, an halo model Evans' logarithmic with $R_{\rm c} = 5$ kpc (identifier A1 in [44]) has been considered for a v_0 value of 170 km/s and halo density at the corresponding maximum value [44]; the form factors parameters and the quenching factors of ^{23}Na and ^{127}I are as in case A of [10]. The *solid* (*dashed*) *curves* delimitate the allowed regions when the channeling effect is (not) included. For simplicity just to point out the impact of the channeling effect, the possible SagDEG contribution to the galactic halo and the presence of the existing Migdal effect – whose effects we discussed in [12] and [13], respectively – are not included here. Moreover, the same considerations reported in [10] still hold

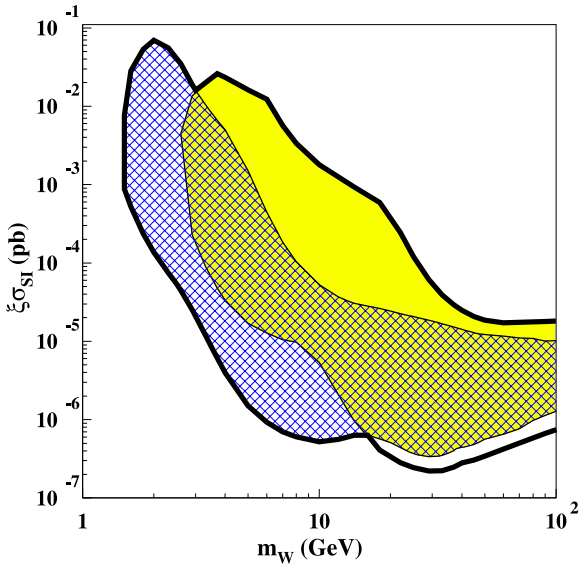

Fig. 8. Region allowed in the $(\xi\sigma_{\rm SI}, m_{\rm W})$ plane in the same model frameworks of [10, 11] for pure SI coupling; just the low mass part of interest for the channeling effect is focused here. The *dotted region* is obtained in absence of channeling effect [10, 11], while the *dashed* one is obtained when accounting for it as described in the text. The *dark line* marks the overal external contour. It is worth to note that the inclusion of other contributions and/or of other uncertainties on parameters and models, such as e.g. the possible SagDEG contribution [12] and the Migdal effect [13] or more favourable form factors, different scaling laws, etc., would further extend the region and increases the sets of the best fit values. For completeness and more see also [10–14]. The same considerations reported in the caption of Fig. 7 hold

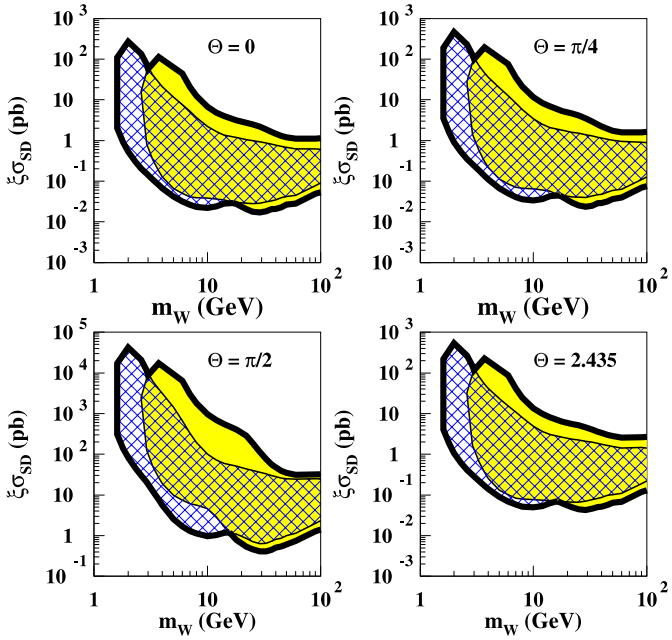

Fig. 9. Examples of slices of the 3-dimensional allowed volume $(\xi\sigma_{\rm SD}, m_{\rm W}, \theta)$ in the same model frameworks of [10, 11] for pure SD coupling; just the low mass part of interest for the channeling effect is focused here. Analogous comments and remarks as those in the captions of Figs. 7 and 8 hold

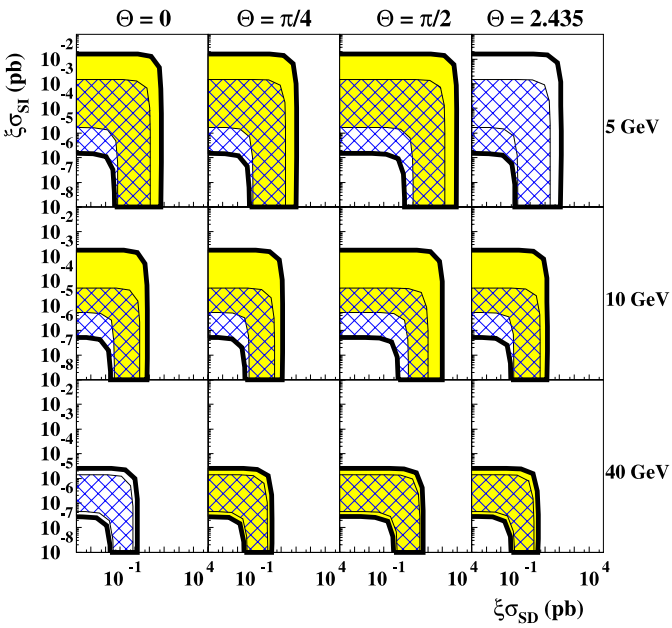

Fig. 10. Examples of slices of the 4-dimensional allowed volume $(\xi\sigma_{\rm SI}, \xi\sigma_{\rm SD}, m_{\rm W}, \theta)$ in the model frameworks considered in [10, 11] for mixed SI and SD coupling; just the low mass part of interest for the channeling effect is focused here. Analogous comments and remarks as those in the captions of Figs. 7 and 8 hold

the corresponding maximum value [44]; the form factors parameters and the quenching factors of ^{23}Na and ^{127}I are as in case A of [10]. The solid (dashed) curves delimitate the allowed regions in the given scenario when the channeling effect is (not) included. As it can be seen, for WIMP masses in the few-20 GeV region the allowed SI region when including the channeling effect is lower than one order of magnitude in cross section.

The subcase of purely SI coupled WIMPs for the scenarios of [10, 11] is shown in Fig. 8, while in Fig. 9 four slices of the 3-dimensional allowed volume $(m_{\rm W}, \xi\sigma_{\rm SD}, \theta)$ for the purely SD case are given as example; the low mass region of interest for the effect is just focused here.

Finally, in the general case of mixed SI and SD coupling one gets, as mentioned above, a 4-dimensional allowed volume $(\xi\sigma_{\rm SI}, \xi\sigma_{\rm SD}, m_{\rm W}, \theta)$. New allowed volume at the given C.L. is present in the GeV region when accounting for the channeling effect. Figure 10 shows few slices of such a volume as examples.

Note that general comments, extensions, etc. already discussed in [10–14] still hold.

6 Conclusions

In this paper the channeling effect of recoiling nuclei induced by WIMP and WIMP-like elastic scatterings in NaI(Tl) crystals has been discussed. Its possible effect in a reasonably cautious modeling has been presented as applied to some given simplified scenarios in corollary quests for the candidate particle for the DAMA/NaI model independent evidence. This further shows the role of the existing uncertainties and of the correct description and modeling of all the involved processes as well as their possible impact in the investigation of the candidate particle. Some of them have already been addressed at some extent, such as the halo modeling [10, 11, 44], the possible presence of non-thermalized components in the halo (e.g. caustics [45] or SagDEG [12] contributions), the accounting for the electromagnetic contribution to the WIMP (or WIMP-like) expected energy distribution [13], candidates other than WIMPs (e.g. [14] and in literature), etc.

Obviously, many other arguments can be addressed as well both on DM candidate particles and on astrophysical, nuclear and particle physics aspects; for more see [10–14] and in literature. In particular, we remind that different astrophysical, nuclear and particle physics scenarios as well as the experimental and theoretical associated uncertainties leave very large space also e.g. for significantly lower cross sections and larger masses.

References

1. J. Lindhard, Phys. Lett. **12**, 126 (1964)
2. R.S. Nelson, N.W. Thompson, Philos. Mag. **8**, 1677 (1963)
3. C.J. Andrean, R.L. Hines, Phys. Rev. **159**, 285 (1967)
4. S.M. Hogg et al., Appl. Phys. Lett. **80**, 4363 (2002)
5. M.M. Bredov, N.M. Okuneva, Dokl. Akad. Nauk. SSSR **113**, 795 (1957)
6. A.M. Rasulov et al., Comp. Mater. Sci. **33**, 148 (2005)
7. A. Baurichter et al., Nucl. Instrum. Methods B **164–165**, 27 (2000)

8. E.M. Drobyshevski, arXiv:0706.3095
9. M. Luntz, R.H. Bartram, Phys. Rev. **175**, 468 (1968)
10. R. Bernabei el al., Riv. Nuovo Cimento **26**, 1 (2003)
11. R. Bernabei el al., Int. J. Mod. Phys. D **13**, 2127 (2004)
12. R. Bernabei et al., Eur. Phys. J. C **47**, 263 (2006)
13. R. Bernabei el al., Int. J. Mod. Phys. A **22**, 3155 (2007)
14. R. Bernabei et al., Int. J. Mod. Phys. A **21**, 1445 (2006)
15. A. Bottino et al., Phys. Rev. D **67**, 063 519 (2003)
16. A. Bottino et al., Phys. Rev. D **68**, 043 506 (2003)
17. A. Bottino et al., Phys. Rev. D **69**, 037 302 (2004)
18. A. Bottino et al., Phys. Lett. B **402**, 113 (1997)
19. A. Bottino et al., Phys. Lett. B **423**, 109 (1998)
20. A. Bottino et al., Phys. Rev. D **59**, 095 004 (1999)
21. A. Bottino et al., Phys. Rev. D **59**, 095 003 (1999)
22. A. Bottino et al., Astropart. Phys. **10**, 203 (1999)
23. A. Bottino et al., Astropart. Phys. **13**, 215 (2000)
24. A. Bottino et al., Phys. Rev. D **62**, 056 006 (2000)
25. A. Bottino et al., Phys. Rev. D **63**, 125 003 (2001)
26. A. Bottino et al., Nucl. Phys. B **608**, 461 (2001)
27. K. Belotsky, D. Fargion, M. Khlopov, R.V. Konoplich, hep-ph/0411093
28. D. Smith, N. Weiner, Phys. Rev. D **64**, 043 502 (2001)
29. D. Smith, N. Weiner, Phys. Rev. D **72**, 063 509 (2005)
30. R. Foot, hep-ph/0308254
31. S. Mitra, Phys. Rev. D **71**, 121 302 (2005)
32. E.M. Drobyshevski et al., arXiv:0704.0982
33. J. Lindhard et al., Mat. Fys. Medd. Dan. Vid. Selsk. **33**, 1 (1963)
34. J.F. Ziegler et al., SRIM – The Stopping and Range of Ions in Matter (2006), http://www.srim.org/
35. J. Lindhard, Mat. Fys. Medd. Dan. Vid. Selsk. **34**, 1 (1965)
36. D.V. Morgan et al., Radiat. Eff. **8**, 51 (1971)
37. S.K. Guharay, slides taken from http://mason.gmu.edu/
38. S.T. Picraux, J.U. Andersen, Phys. Rev. **186**, 267 (1969)
39. R. Bernabei el al., Phys. Lett. B **389**, 757 (1996)
40. H. Chagani et al., arXiv:physics/0611156
41. E. Simon et al., Nucl. Instrum. Methods A **507**, 643 (2003)
42. R. Bernabei et al., Nuovo Cim. A **112**, 545 (1999)
43. R. Bernabei et al., Eur. Phys. J. C **18**, 283 (2000)
44. P. Belli et al., Phys. Rev. D **66**, 043 503 (2002)
45. F.S. Ling, P. Sikivie, S. Wick, Phys. Rev. D **70**, 123 503 (2004)